

# Computational Study of the Gas-Phase Thermal Degradation of Perfluoroalkyl Carboxylic Acids

Published as part of *The Journal of Physical Chemistry* virtual special issue "Combustion in a Sustainable World: From Molecules to Processes".

Claude-Bernard Paultre, Alexander M. Mebel,\* and Kevin E. O'Shea\*



Cite This: *J. Phys. Chem. A* 2022, 126, 8753–8760



Read Online

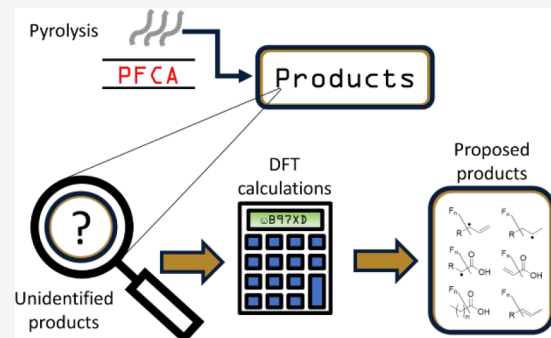
ACCESS |

Metrics & More

Article Recommendations

Supporting Information

**ABSTRACT:** Perfluoroalkyl carboxylic acids (PFCAs) are persistent and ubiquitous pollutants. Environmental remediation is often achieved by absorption on matrices followed by high-temperature thermal treatment to desorb and decompose the PFCAs. Detailed product studies of the thermal degradation of PFCAs have been hampered by the complex nature of product mixtures and associated analytical challenges. On the basis of high-level computational studies, we propose reaction pathways and mechanisms for the high-temperature mineralization of a series of linear PFCAs with a backbone length from C-4 to C-8. The favored initial reaction pathways are nonselective C–C bond homolytic cleavages (with bond dissociation energies of  $\sim 75$ – $90$  kcal/mol), resulting in carbon-centered radicals which can undergo  $\beta$ -scissions ( $E_a \approx 30$ – $40$  kcal/mol) which can be preceded by F atom shifts ( $E_a \approx 30$ – $45$  kcal/mol). In competing barrierless processes, the carbon-centered radicals can lose  $^{\bullet}\text{F}$ , resulting in the formation of volatile perfluoroalkenes ( $\Delta H \approx 50$ – $80$  kcal/mol). A variety of competing fragmentation processes yield shorter chain perfluorinated PFCAs, isomeric alkenes, alkenoic acids, alkyl, and alkyloic acid radicals. The results provide the energetics for primary, secondary, and tertiary reaction products and insight into the fundamental understanding of the pyrolytic pathways of PFCAs leading to their mineralization.



## INTRODUCTION

Perfluoroalkyl substances (PFAS) are a class of contaminants raising serious safety concerns throughout the world.<sup>1–3</sup> Their intrinsic properties make them exceptional candidates for a tremendous number of applications, including use as fire-fighting foams and nonstick coatings for cooking and food packaging. These same properties also make them extremely resistant to natural degradation and standard remediation processes.<sup>4</sup> Thus, PFAS are often referred to as *Forever Chemicals*. In the United States, these compounds have been ubiquitously detected in blood samples.<sup>5,6</sup> PFAS are also present across the globe even in the most remote parts of the planet including our polar regions.<sup>7,8</sup>

Numerous groups have studied the application of conventional and nonconventional water treatments on PFAS. Techniques including membrane filtration and sonolysis have shown promise in the challenge for remediation of PFAS with various levels of success.<sup>9</sup> PFAS-contaminated membranes, activated carbon, and ion exchange resins need to be regenerated. High-temperature pyrolysis processes are commonly used to regenerate PFAS-laden adsorbents.<sup>9</sup> Unfortunately, there is limited knowledge about the nature and toxicity of the PFAS thermal degradation pathways and byproducts.

Although product elucidation and mechanistic schemes have been proposed for thermally induced PFAS fragmentations,<sup>10–18</sup> previous reports are primarily limited to the initial steps of the degradation and carried only on a limited number of PFAS. Bond dissociation energies (BDEs) and thermodynamic data have been calculated for the initial steps for several classes of PFAS.<sup>11,12,17,19–24</sup> A detailed study of the pyrolytic processes leading to mineralization has yet to be reported.

Perfluoroalkyl carboxylic acids (PFCAs) are a problematic subclass of PFAS that includes the legacy compound perfluorooctanoic acid (PFOA). Here, detailed computational studies were run to determine the energetics of competing thermal degradation pathways, from the initial homolytic bond cleavage to the mineralization of PFCAs.

Received: September 8, 2022

Revised: October 27, 2022

Published: November 14, 2022



## ■ COMPUTATIONAL METHODS

Density functional theory (DFT) calculations were carried out using the  $\omega$ B97xD functional and the 6-311+G(d,p) basis set.<sup>25</sup> In some cases, the G3(CC,MP2) model chemistry approach<sup>26,27</sup> was employed to refine single-point energies at the  $\omega$ B97xD/6-311+G(d,p)-optimized geometries. The Gaussian 09 software package was employed in the DFT and the second-order Møller–Plesset perturbation theory (MP2) ab initio calculations.<sup>28</sup> The MOLPRO software package<sup>29</sup> was utilized in the coupled-cluster calculations with single and double excitations and perturbative treatment of triple excitations (CCSD(T)).

The initial structures of PFCAs and their pyrolysis radical products formed by homolytic cleavages of various bonds were optimized, and the energies of the homolytic bond cleavages were calculated.

The energetics of various pyrolytic pathways were investigated. The transition state (TS) structures were optimized for each reaction pathway featuring a distinct barrier, in particular, for  $\beta$ -scissions and F atom migrations. For example, for  $\beta$ -scissions, bonds subject to cleavage were elongated by approximately a factor of 1.3, and the resulting Cartesian coordinates were used as the initial estimate of the TS geometry. In most cases, the 30% increase in the bond length gives a guessed structure that converges to a TS during geometry optimization. The connections of the TS structures with appropriate local minima were subsequently verified by using intrinsic reaction coordinate (IRC) calculations<sup>30,31</sup> or by visualization of the normal mode corresponding to the imaginary frequency using Avogadro.<sup>32,33</sup>

## ■ RESULTS AND DISCUSSION

Detailed computational studies were carried out for linear PFCAs containing from 4 to 8 carbon atoms in the alkyl chain (Figure 1). BDEs critical for the assessment of homolytic

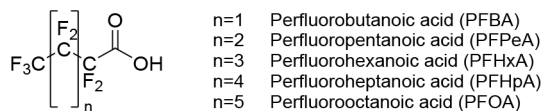


Figure 1. Representative perfluoroalkyl carboxylic acids.

reaction pathways initiated during pyrolysis were calculated for all C–C and C–F bonds for these PFCAs. The C–O bonds of the carboxylic headgroup have a higher bond order (in the case of  $C=O$ ) or higher bond strengths (112 kcal/mol for COO–H of perfluoropentanoic acid, ~109 kcal/mol for the CO–OH bonds of carboxylic acids)<sup>18,34</sup> and thus were not considered.

The BDEs were determined from the difference between the zero-point energy (ZPE)-corrected electronic energy of the initial molecule and the sum of the corrected energies of the radical products. PFCAs are strong acids ( $pK_a \approx 0$ ) and can exist in deprotonated or ionized form under environmental conditions ( $pH \approx 6–8$ ).<sup>21,35</sup> With this in mind, the BDEs for the C–C and C–F bonds of the carboxylic acid and the carboxylate forms are calculated and summarized below. The BDEs are significantly different for the acid and the carboxylate forms. The trends in BDEs presented in Tables 1–4 are summarized in two paragraphs below making the following key points.

The C–C BDEs for the carboxylic acids are from 73.3 to 87.9 kcal/mol, generally lower compared to the carboxylate

Table 1. C–C Bond Dissociation Energies (in kcal/mol) of PFCAs

chain length	bond						
	a	b	c	d	e	f	g
4	82.5	75.8	86.9				
5	81.1	73.3	80.6	85.3			
6	82.8	74.5	80.7	81.6	86.8		
7	82.9	75.0	80.6	80.5	81.9	87.4	
8	82.9	75.1	81.0	80.4	80.7	82.4	87.9

Table 2. C–C Bond Dissociation Energies (in kcal/mol) of PFCA Carboxylate Ions

chain length	bond						
	a	b	c	d	e	f	g
4	90.2	88.1	89.1				
5	90.7	87.5	84.7	88.1			
6	91.5	87.8	83.9	83.5	87.4		
7	91.8	88.4	84.0	82.5	82.7	86.8	
8	91.9	88.7	84.5	82.5	81.6	82.0	86.6

Table 3. C–F Bond Dissociation Energies (in kcal/mol) of PFCAs

chain length	fluorine position							
	2	3	4	5	6	7	8	
4	101.8	109.3	116.8					
5	100.8	106.7	107.1	116.8				
6	102.3	107.2	106.1	107.8	117.0			
7	101.3	106.7	105.9	106.4	109.0	117.0		
8	102.3	108.5	106.0	106.2	106.3	107.7	117.5	

Table 4. C–F Bond Dissociation Energies (in kcal/mol) of PFCA Carboxylate Ions

chain length	fluorine position							
	2	3	4	5	6	7	8	
4	107.8	108.2	118.6					
5	108.0	106.0	108.2	118.4				
6	107.2	105.8	106.7	108.0	117.9			
7	107.3	105.7	106.3	106.4	107.9	118.4		
8	108.2	105.8	106.2	106.1	107.8	107.9	118.3	

ions which range from 81.6 to 91.9 kcal/mol. The acid forms exhibit preference for cleavage  $\beta$  to the headgroup (bond b) with BDEs = 74  $\pm$  2 kcal/mol regardless of the chain length. The bond between the  $sp^3$ - and the  $sp^2$ -hybridized C atoms (C<sub>sp3</sub>–C<sub>sp2</sub>, bond a) in acid form have higher C–C BDEs with nearly identical values (81.1–82.9 kcal/mol) and are

independent of the chain length. The remaining internal C–C bonds have BDEs  $\approx$  80–82 kcal/mol, while terminal C–C bonds have BDEs  $\approx$  85–87 kcal/mol. In comparison to acid forms, the preference for the  $\beta$  cleavage (bond b) is eliminated for the carboxylate forms, internal C–C bond cleavages are energetically favored by  $\sim$ 5–10 kcal/mol, terminal C–C cleavages are slightly disfavored ( $\sim$ 87–89 kcal/mol), and C<sub>sp<sup>3</sup></sub>–C<sub>sp<sup>2</sup></sub> bonds (bond a) have the highest BDEs ( $\sim$ 90–92 kcal/mol).

In all cases, the C–F bonds are stronger than the C–C bonds. The C–F BDEs are generally lower for the carboxylic acids, 100.8–117.5 kcal/mol, compared to the carboxylate forms which range from 105.7 to 118.6 kcal/mol. The acid forms exhibit preference for C–F cleavage  $\beta$  to the headgroup (F in position 2) with BDEs = 101  $\pm$  1 kcal/mol regardless of the chain length. The remaining internal C–F bonds have BDEs  $\approx$  106–109 kcal/mol with terminal C–F bonds being the strongest,  $\sim$ 117  $\pm$  0.5 kcal/mol. In comparison to acid forms, the preference for the  $\beta$  cleavage (F in position 2) is eliminated for the carboxylate ions; the internal C–F bond cleavages are comparable at  $\sim$ 106–108 kcal/mol, and terminal C–F bonds have the highest BDEs of 118  $\pm$  0.5 kcal/mol.

We further rationalize the observed trends in the BDEs considering that the BDEs reflect the stability of the products. Cleavage of the terminal C–C bond generates carbon-centered radicals, the trifluoromethyl radical, and a primary radical,  $^{\bullet}\text{CF}_3$  +  $^{\bullet}\text{CF}_2\text{R}$ . Carbon-centered radicals are inherently electron deficient by definition using the octet rule. The presence of powerful electron-withdrawing F atoms further destabilizes carbon-centered radicals. With this in mind, the strongly electron-deficient  $^{\bullet}\text{CF}_3$  due to three powerful electron-withdrawing F atoms will be among the least stable products for homolytic bond cleavage pathways of PFCAs. Thus, homolytic C<sub>sp<sup>3</sup></sub>–C<sub>sp<sup>3</sup></sub> cleavage pathways yielding  $^{\bullet}\text{CF}_3$  have higher BDEs.<sup>36</sup> The C–C BDEs for the formation of the trifluoromethyl radical from the acid and the carboxylate forms are similar (87  $\pm$  2 kcal/mol). However, in the case of the carboxylate forms, the strongest C–C bond is C<sub>sp<sup>3</sup></sub>–C<sub>sp<sup>2</sup></sub> (Table 2). While F atoms destabilize carbon-centered radicals, the hybridization of the carbon is also an important consideration in general.  $^{\bullet}\text{C}_{\text{sp}^3}$  is more stable than  $^{\bullet}\text{C}_{\text{sp}^2}$ . Thus, the carbon dioxide radical anion is even less stable than the trifluoromethyl radical. When the resulting radical from the carboxylate form is  $\alpha$  (cleavage of bond b) to the headgroup, the BDE increases by  $\sim$ 5–10 kcal/mol compared to the same cleavage from the carboxylic acid forms. Resonance is another key feature in the stability of the radicals. The delocalization of the radical center due to resonance generally increases the overall stability of the radical product. This suggests that the anionic charge of the carboxylate ion destabilizes the radical by mostly preventing resonance of the unpaired electron to the C=O group. The difference between the BDEs from the carboxylate and carboxylic acid forms decreases to less than 5 kcal/mol as one moves two or more C atoms away from the headgroup.

**Method Validation and Comparison with the Literature.** The calculations are further verified using the composite G3(CC,MP2) method for PFBA (Table 5). With a mean absolute error of 6.3 kcal/mol and a mean relative error of 6.4%, the  $\omega$ B97XD method predictions of the BDEs for the C–F bond are accurate within  $\sim$ 5 kcal/mol and within  $\sim$ 4–9 kcal/mol for the C–C bonds (Table 5). The maximal error is

**Table 5. Bond Dissociation Energies (in kcal/mol) Calculated at the  $\omega$ B97XD and G3(CC,MP2) Levels**

bond	method		$\Delta E$
	$\omega$ B97XD/6-311+G(d,p)	G3(CC,MP2) <sup>a</sup>	
a	82.5	87.1	4.6
b	75.8	84.9	9.1
c	86.9	94.6	7.7
2	101.8	107.0	5.2
3	109.3	115.0	5.7
4	116.8	122.0	5.2

<sup>a</sup>G3(CC,MP2), optimized structures from  $\omega$ B97XD/6-311+G(d,p).

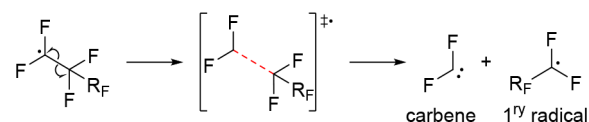
9.1 kcal/mol. These errors are in agreement with reported errors for other hybrid DFT methods.<sup>37</sup>

The BDEs computed in the present study are compared with the literature data mostly obtained using the B3LYP functional and taking into account solvent effects (Tables S1–S5 in the Supporting Information).<sup>10–12,22–24</sup> There is a general agreement between the values obtained for the C–C BDEs in the carboxylic acid forms and the C–F BDEs in the carboxylate forms. The C–C BDEs of the carboxylate forms show differences of 3–12 kcal/mol, suggesting that the solvent effects are more pronounced for the charged carboxylate forms. Altarawneh calculated the unimolecular dissociation of PFBA using a G3 method.<sup>17</sup> When compared to the data obtained here at the G3(CC,MP2) level, the differences do not exceed 1 kcal/mol (Table S3).

**Secondary Degradation of the Radicals Created by Homolytic Cleavage. Possible Reactions of the Radicals.** Our results illustrate significant differences in the BDEs of the acid and carboxylates across the studied PFCAs while also demonstrating clear structure–activity relationships (see below). These BDEs are in general agreement with literature reports at various computational levels, and we further verified data employing higher level computations. There are, however, very limited studies on the subsequent reaction pathways of the carbon-centered radicals produced from homolytic cleavages of PFCAs. Carbon-centered radicals typically react via specific competing reaction pathways, notably  $\alpha$ - and  $\beta$ -scissions, atomic shifts, or fragment losses as outlined below. Note that F atoms are not explicitly labeled in the schemes presented below unless this is needed for clarity.

**$\alpha$ -Scission.** Homolytic fragmentation at the radical center generates a highly reactive carbene (Scheme 1). The carbene

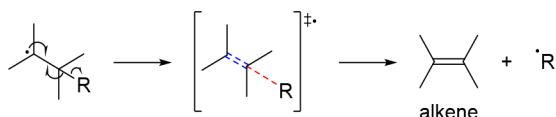
**Scheme 1. General Mechanism of  $\alpha$ -Scission**



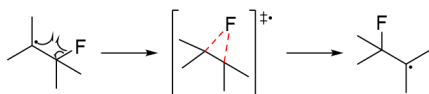
can exist as a singlet or triplet spin ground state depending on structural and electronic factors. Fluorine-substituted carbenes typically have a singlet ground state.

**$\beta$ -Scission.** Loss of a substituent vicinal to the carbon-centered radical generates a double bond (Scheme 2).<sup>38</sup>

**1,2-Shift.** The 1,2-shift of the F atom to the carbon radical center is often energetically favored (Scheme 3).<sup>36</sup>

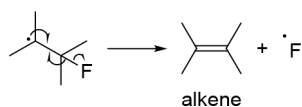
Scheme 2. General Mechanism of  $\beta$ -Scission

## Scheme 3. General Mechanism of 1,2-Fluorine Shift



**F Loss.** The C–F bond adjacent to the carbon-centered radical can be cleaved to form a new C–C  $\pi$  bond (Scheme 4).

## Scheme 4. General Mechanism of Fluorine Loss



Despite repeated attempts to identify the reaction pathways and the TS leading to the loss of  $\cdot\text{F}$  via  $\beta$ -scission, the lack of convergence suggests a barrierless process without a TS. The resulting double bond can be *cis* or *trans*.

A variety of other pathways for transformation of radicals were investigated, but the energetics indicated that such processes are not competitive. The activation energies ( $E_a$ ) for  $\beta$ -scission,  $\cdot\text{F}$  loss, and F atom shift of perfluoroalkyl and perfluoroalkyloic acid radicals were determined computationally as detailed in Tables 6–9. Potential energy diagrams for the decomposition reaction of the radicals studied here are presented in the Supporting Information (Figures S2–S17).

Table 6. Activation Energies (in kcal/mol) for  $\beta$ -Scissions of Perfluoroalkyl Radicals

chain length	position of radical			
	1	2	3	4
3	41.7 <sup>a</sup>			
4	37.3	37.4 <sup>a</sup>		
5	35.6	33.8	37.9 <sup>a</sup>	
6	34.9	32.3	34.1/37.8 <sup>a</sup>	
7	35.4	32.1	32.3/36.1 <sup>a</sup>	33.7

<sup>a</sup>Loss of  $\cdot\text{CF}_3$  radical.

To the best of our knowledge,  $\beta$ -scissions have previously been reported for perfluoroalkoxy radicals via a photocatalytic process in the presence of oxygen.<sup>39</sup> The  $\beta$ -scission mechanism is also in line with experimental data in the literature where perfluoroethylene, among other perfluoroalkenes, has been detected as a product of the pyrolysis of PFAS.<sup>40</sup> Experimental mass spectrometry data for the fragmentation of PFOA suggest F shifts being the kinetic products compared to  $\beta$ -scissions.<sup>41</sup> The energies calculated here for F shifts and  $\beta$ -scissions are similar, suggesting both processes occur.

The  $\beta$ -scissions of the perfluoroalkyl radicals yield shorter chain radicals and perfluoroalkenes with relatively low  $E_a$  ( $\sim 32$ –42 kcal/mol) (Table 6). The  $\beta$ -scissions presented

Table 7. Activation Energies (in kcal/mol) for the F Shifts of Perfluoroalkyl Radicals

chain length	shift in the unpaired electron position		
	1 to 2	2 to 3	3 to 4
3	35.8		
4	37.4		
5	35.5	44.3	
6	35.4	38.9	
7	35.4	39.3	39.4

Table 8. Activation Energies (in kcal/mol) for the  $\beta$ -Scissions of Perfluoroalkyloic Acids Radicals

chain length	position of radical						
	2	3	4	5	6	7	
3		38.4 <sup>b</sup>					
4	38.7 <sup>a</sup>	33.2 <sup>b</sup>	33.2 <sup>d</sup>				
5	34.1 <sup>c</sup>	37.1 <sup>a</sup>	29.5 <sup>d</sup>	35.1 <sup>b</sup>			
		33.4 <sup>b</sup>					
6	32.1 <sup>c</sup>	32.8 <sup>c</sup>	38.2 <sup>a</sup>	32.6 <sup>b</sup>	33.8 <sup>b</sup>		
		32.9 <sup>b</sup>	31.2 <sup>d</sup>				
7	32.5 <sup>c</sup>	32.0 <sup>c</sup>	34.7 <sup>c</sup>	38.0 <sup>a</sup>	20.5 <sup>b</sup>	33.5 <sup>b</sup>	
		32.1 <sup>b</sup>	31.3 <sup>d</sup>	33.0 <sup>b</sup>			

<sup>a</sup>Loss of  $\cdot\text{CF}_3$  radical. <sup>b</sup>Loss of perfluoroalkyloic acid radicals. <sup>c</sup>Loss of perfluoroalkyl radicals. <sup>d</sup>Loss of perfluoroethyloic acid radical.

herein lead to the formation of primary radicals and/or trifluoromethyl radicals (designated with footnote a). Relatively small energy differences of  $<10$  kcal/mol are observed among the different reaction pathways.

Activation energies of  $\sim 35$  kcal/mol were calculated for F shifts of the perfluoroalkyl radicals resulting in a primary-to-secondary radical shift and  $\sim 40$  kcal/mol for secondary-to-secondary radical shifts (Table 7). The slight energy differences observed between these processes are consistent with the secondary radicals being more stable, thus requiring higher energy to reach the TS leading to the product. Our results are in accordance with Hoomissen and Vyas's findings reported for shorter chain perfluoroalkyl radicals (linear radical with a backbone from C-3 to C-5).<sup>36</sup>

In the case of the  $\beta$  elimination of  $\cdot\text{F}$  from perfluoroalkyl radicals, the reaction does not have a TS (no  $E_a$ ). The enthalpies were used to compare the energetics of competing processes. The reaction enthalpies for loss of  $\cdot\text{F}$  are  $\sim 55$ –60 kcal/mol except when a secondary radical results in a terminal alkene, in which case the enthalpy is slightly higher,  $\sim 65$  kcal/mol (Table S6). The trifluoromethyl radical can only go through an  $\alpha$  elimination of  $\cdot\text{F}$ , and the enthalpy of this reaction (83.4 kcal/mol) is higher than the  $E_a$  of  $\beta$ -scissions for the other radicals. This suggests that  $\beta$ -scissions are more probable reaction pathways, consistent with the literature on the thermolysis of carbon-based polymers, where higher temperatures are required for the  $\alpha$ -scission pathways to be competitive.<sup>42</sup>

The energies for pathways yielding *cis* and *trans* alkenes are the same within computational accuracy; thus, no selectivity is anticipated (Table S9). The complete table of reaction enthalpies for the loss of  $\bullet\text{F}$  in perfluoroalkyl radicals can be found in the Supporting Information (Table S6).

The  $\omega$ -perfluoroalkyloic acid radicals (Figure 2), where the unpaired electron is at the terminal C, follow the same reaction pathways predicted for the perfluoroalkyl radicals.

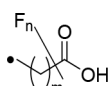


Figure 2. Structure of the  $\omega$ -perfluoroalkyloic acid radicals

The activation energies for  $\beta$ -scissions, with loss of trifluoromethyl radical (footnote a in Table 8) ( $\sim 38$  kcal/mol), are modestly higher compared to other perfluoroalkyl radicals ( $\sim 33$  kcal/mol). The perfluoroalkyloic acid radicals that fragment by loss of a perfluoroethyloic acid radical stabilized by resonance have the lowest observed  $E_a$  of  $\sim 31$  kcal/mol (footnote d in Table 8).

The activation energy for a primary to secondary (terminal to internal) radical shift in the case of perfluoroalkyloic acid radicals is lower than the secondary to secondary shifts by  $\sim 5$  kcal/mol (Table 9). The F shift from C-3 to a carbon-centered

Table 9. Activation Energies (in kcal/mol) for the F Shifts of Perfluoroalkyloic Acid Radicals



chain length	shift in the unpaired electron position				
	3 to 2	4 to 3	5 to 4	6 to 5	7 to 6
3	30.1				
4	34.4	32.6			
5	33.8	36.9	34.7		
6	35.0	36.8	40.4	34.4	
7	33.1	40.8	40.7	39.4	33.7

radical at C-2 has a lower  $E_a$  than other secondary to secondary shifts because a resonance-stabilized radical is produced. Several attempts to calculate the scission resulting in the formation of a ketene and the loss of a hydroxyl radical were unsuccessful, suggesting such pathway is not competitive.

To the best of our knowledge, the  $\bullet\text{F}$  losses in these perfluorinated radicals have not been previously reported. The enthalpy for the loss of  $\bullet\text{F}$  in the perfluoroalkyloic acid radicals is  $\sim 50$ – $60$  kcal/mol. The formation of terminal perfluoroalkenoic acids has a higher enthalpy ( $\sim 68$  kcal/mol) when the starting structure is a secondary radical compared to primary radicals (Table S7). The difference in enthalpies reflects the stability of the primary versus the secondary radical. The enthalpies for  $\bullet\text{F}$  loss from C-3 radicals to form perfluoroalk-2-enoic acids are the lowest among the enthalpies for  $\bullet\text{F}$  losses of a perfluoroalkyloic acid radical, consistent with the increase in stability due to the conjugated  $\pi$  system in the perfluoroalkenoic acid formed. The carbon-centered C-2 radicals are also resonance stabilized, and the effect of resonance stabilization is less pronounced. The complete table of reaction enthalpies for the loss of  $\bullet\text{F}$  in

perfluoroalkyloic acid radicals can be found in the Supporting Information (Table S7).

**Fate of the Perfluoroalkenes.** Perfluoroalkenes are stable and commercially available in gas or liquid form. Perfluoroalkenes are one of the identified byproducts of low-temperature decomposition of PFCA salts along with carbon dioxide.<sup>16,43</sup> The simplest member of this group, perfluoroethylene (tetrafluoroethylene), is the monomer of polytetrafluoroethylene (PTFE or Teflon). Experimental data on the thermal degradation exist for perfluoropropene<sup>44</sup> and perfluoroethylene and suggest rearrangement or polymerization,<sup>43</sup> but many of the reaction pathways and products are unidentified.<sup>43</sup> Computational and experimental data exist for the C=C BDE of perfluoroethylene and are in agreement with our results below.<sup>45</sup>

The C–C and C–F BDEs for the perfluoroalkenes were calculated, and the magnitude is similar to the BDEs for PFCA (Tables 1, 2, S11, and S12). The reaction pathways and byproducts of the degradation of the perfluoroalkenes were analyzed for subsequent degradation pathways.

**Adiabatic and Diabatic Bond Dissociation Energies.** Breaking the C=C bonds of the perfluoroalkenes can follow a diabatic or an adiabatic cleavage pathway. An adiabatic bond cleavage calculation analyzes the reactants and products on their ground state, while a diabatic cleavage considers the bonding configuration of the reactant to define that of the products. Difluorocarbene is a ground-state singlet that does not have the correct spin configuration to form the  $\sigma$  and  $\pi$  bond of the perfluoroethylene.<sup>45,46</sup> The diabatic BDE will then be of a singlet state double bond giving triplet carbene (Figure 3). The BDEs obtained for the perfluoroethylene are in accordance with Feller et al.<sup>45</sup>

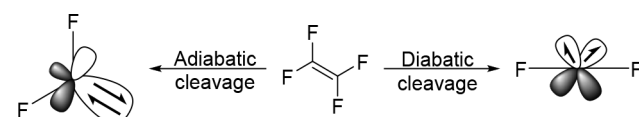


Figure 3. Diabatic and adiabatic cleavage products.

The C–F bonds ( $\sim 96.7$ – $133.6$  kcal/mol) are stronger than the C–C bonds ( $\sim 74.7$ – $105.5$  kcal/mol) of the perfluoroalkenes (Tables S11 and S12). The weakest C–F bonds ( $\sim 96.7$ – $99.3$  kcal/mol) and C–C bonds ( $\sim 74.7$ – $76.2$  kcal/mol) lead to a resonance-stabilized perfluoroalk-1-en-3-yl radical (Figure 4). The cleavage of the C–C bond yielding a

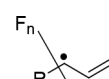


Figure 4. Structure of the perfluoroalk-1-en-3-yl radicals.

trifluoromethyl radical (or an  $\bullet\text{F}$  with a primary radical from a C–F bond rupture) and the resonance-stabilized perfluoroprop-1-en-3-yl radical requires 5–10 kcal/mol more compared to analogous cleavage in longer chain perfluoroalkenes as the products that are formed in that case are less stable. Among the strongest bonds are the  $\text{C}_{\text{sp}2}$ –F (BDE  $\approx 122$ – $123$  kcal/mol), which will yield generally the least stable vinyl radical products. Blanksby and Allison have shown a similar trend for alkanes where there is an  $\sim 30$  kcal/mol difference between the sp-hybridized C bound to H ( $\text{C}_{\text{sp}}\text{–H}$ ) and the  $\text{C}_{\text{sp}3}\text{–H}$  BDE.<sup>47</sup>

The perfluoroalkenes undergo predominantly fragmentations at the C–C bonds (Tables S11 and S12). The alkenes with at least 4 carbons form perfluoroalkenyls with loss of a perfluoroalkyl radical. Perfluoropropene has C–C BDEs similar to C–F BDEs, making the compound stable enough until there is enough energy to break even the C–F bonds. In the case of perfluoroethene, the C=C BDE is higher than the C–F BDEs by more than 40 kcal/mol, suggesting the need for more energy to break this compound.

The perfluoroalkenyl radicals are subject to  $\beta$ -scission (Table 10), F shift (Table 11), or  $^{\bullet}\text{F}$  loss (Table S8). The

**Table 10. Activation Energies (in kcal/mol) for the  $\beta$ -Scissions of Perfluoroalkenyl Radicals**

chain length	position of radical			
	3	4	5	6
3		67.8		
4	42.5 <sup>a</sup>	48.2	34.1	
5	39.9	37.9 <sup>a</sup> /67.8	29.7	36.7

<sup>a</sup>Loss of  $^{\bullet}\text{CF}_3$  radical.

**Table 11. Activation Energies (in kcal/mol) for the F Shifts of Perfluoroalkenyl Radicals**

chain length	shift in the unpaired electron position		
	4 to 3	5 to 4	6 to 5
3	30.1		
4	32.5	35.4	
5	32.8	39.1	35.4

perfluoroalkenyl radicals follow analogous processes as the perfluoroalkyl radicals: Activation energies reflect relative product stabilities, with the most stable being molecular species and/or a resonance-stabilized radical, with  $E_a \approx 30\text{--}40$  kcal/mol. The formation of a vinyl radical ( $\text{C}_{\text{sp}^2}$ -centered radical) requires the highest energy ( $\sim 50\text{--}70$  kcal/mol).

The  $E_a$  values for the F shifts are about the same within the series ( $\sim 33\text{--}35$  kcal/mol). The  $^{\bullet}\text{F}$ -loss reactions show insignificant difference between *cis* and *trans* isomers (Table S13). With reaction enthalpies of  $\sim 55\text{--}70$  kcal/mol, the  $^{\bullet}\text{F}$  losses show the same trend as described previously: it takes more energy to form a terminal alkene from a secondary radical than a primary one; when the diene obtained is resonance stabilized, the enthalpy is lower; the enthalpy increases (by  $\sim 10$  kcal/mol) when the final product and the starting radical are resonance stabilized compared to when the starting radical is not stabilized. The complete table of reaction enthalpies for the loss of  $^{\bullet}\text{F}$  in perfluoroalkyl radicals can be found in the Supporting Information (Table S8).

## CONCLUSIONS

The study of the homolytic bond cleavages in PFCAs in acid and anionic forms followed by secondary rearrangement and decomposition reactions detailed above helps to fill a knowledge gap in the literature and contributes to understanding how other products can be formed from the

degradation processes of the primary radical products in pyrolysis.

In summary, the favored initial degradation pathways are nonselective C–C bond homolytic cleavages (with bond dissociation energies of  $\sim 75\text{--}90$  kcal/mol). Next, the perfluoroalkyl radicals can go through competing reaction pathways, including fluorine shifts or losses and  $\beta$ -scissions, and usually end up forming perfluoroalkenes and shorter chain radicals such as perfluoromethyl or perfluoroethyl. The calculations have shown that the same reactions hold for the perfluoroalkyloic acid radicals. These end up forming perfluoroalkenoic acids, perfluoroalkenes, and shorter chain perfluoroalkyl radicals. With regard to larger linear PFCAs with  $n > 5$ , our results here for smaller species indicate that an increase of the carbon chain length had a minimal effect on the BDEs of the medial C–C and C–F bonds. Similarly, the secondary degradations of the generated radicals are energetically and mechanistically comparable. This suggests that the longer chains would behave in a similar fashion.

The energy needed for the first bond cleavage in PFCAs is enough to degrade the byproducts of the reaction. The tertiary degradation processes were analyzed for the perfluoroalkenes. The results showed that perfluoroalkadienes form along with shorter perfluoroalkenes and perfluoroalkyl radicals. The studied reaction mechanisms and energetics provide insight into the fundamental understanding of the pyrolytic pathways of PFCAs leading to their mineralization. The mechanisms presented herein could be used in future calculations of pertinent reaction rate constants and in kinetic modeling aimed to determine the competitiveness of these reactions against other proposed mechanisms. While typical pyrolysis conditions might not be directly applicable to environmental degradation conditions, the products identified here might help in the identification of byproducts of other degradation techniques and should prove helpful in the development of more efficient techniques for the removal of these *Forever Chemicals* from the environment.

## ASSOCIATED CONTENT

### Supporting Information

The Supporting Information is available free of charge at <https://pubs.acs.org/doi/10.1021/acs.jpca.2c06437>.

Nomenclature used for the radicals; potential energy diagrams of the studied radical decomposition reactions; comparison tables between BDEs computed here and in the literature; enthalpies of the F-loss reactions from the radicals studied in this work; energy differences between the *cis*- and the *trans*-perfluoroalkenes, alkenoic acids, and alkadienes; BDE for the perfluoroalkenes (PDF)

## AUTHOR INFORMATION

### Corresponding Authors

Alexander M. Mebel – Department of Chemistry and Biochemistry, Florida International University, Miami, Florida 33199, United States;  [orcid.org/0000-0002-7233-3133](https://orcid.org/0000-0002-7233-3133); Email: [mebel@fiu.edu](mailto:mebel@fiu.edu)

Kevin E. O’Shea – Department of Chemistry and Biochemistry, Florida International University, Miami, Florida 33199, United States;  [orcid.org/0000-0002-9695-4321](https://orcid.org/0000-0002-9695-4321); Phone: 305-348-3968; Email: [osheak@fiu.edu](mailto:osheak@fiu.edu)

**Author**

**Claude-Bernard Paultre** – Department of Chemistry and Biochemistry, Florida International University, Miami, Florida 33199, United States

Complete contact information is available at:  
<https://pubs.acs.org/10.1021/acs.jpca.2c06437>

**Author Contributions**

C.P. ran the calculations included in this article under the supervision of A.M.M. and K.E.O. A.M.M. ran the CCSD(T) single-point calculations. The manuscript was written through contributions of all authors. All authors have given approval to the final version of the manuscript.

**Notes**

The authors declare no competing financial interest.

**ACKNOWLEDGMENTS**

This work was funded by the National Science Foundation (NSF 1805718). The authors acknowledge the Instructional & Research Computing Center (IRCC, web <http://ircc.fiu.edu>) at Florida International University for providing HPC computing resources. The authors also thank Dr. Detlef Knappe for his feedback.

**REFERENCES**

- (1) Pelch, K. E.; Reade, A.; Wolffe, T. A. M.; Kwiatkowski, C. F. PFAS Health Effects Database: Protocol for a Systematic Evidence Map. *Environ. Int.* **2019**, *130*, 104851.
- (2) Domingo, J. L.; Nadal, M. Human Exposure to Per- and Polyfluoroalkyl Substances (PFAS) through Drinking Water: A Review of the Recent Scientific Literature. *Environ. Res.* **2019**, *177*, 108648.
- (3) Ghisi, R.; Vamerali, T.; Manzetti, S. Accumulation of Perfluorinated Alkyl Substances (PFAS) in Agricultural Plants: A Review. *Environ. Res.* **2019**, *169*, 326–341.
- (4) Ross, I.; McDonough, J.; Miles, J.; Storch, P.; Thelakkat Kochunarayanan, P.; Kalve, E.; Hurst, J.; S. Dasgupta, S.; Burdick, J. A Review of Emerging Technologies for Remediation of PFASs. *Remediation* **2018**, *28*, 101–126.
- (5) Calafat, A. M.; Wong, L. Y.; Kuklenyik, Z.; Reidy, J. A.; Needham, L. L. Polyfluoroalkyl Chemicals in the U.S. Population: Data from the National Health and Nutrition Examination Survey (NHANES) 2003–2004 and Comparisons with NHANES 1999–2000. *Environ. Health Perspect.* **2007**, *115*, 1596–1602.
- (6) Calafat, A. M.; Kato, K.; Hubbard, K.; Jia, T.; Botelho, J. C.; Wong, L. Y. Legacy and Alternative Per- and Polyfluoroalkyl Substances in the U.S. General Population: Paired Serum-Urine Data from the 2013–2014 National Health and Nutrition Examination Survey. *Environ. Int.* **2019**, *131*, 105048.
- (7) Del Vento, S.; Halsall, C.; Gioia, R.; Jones, K.; Dachs, J. Volatile Per- and Polyfluoroalkyl Compounds in the Remote Atmosphere of the Western Antarctic Peninsula: An Indirect Source of Perfluoroalkyl Acids to Antarctic Waters? *Atmos. Pollut. Res.* **2012**, *3*, 450–455.
- (8) Verreault, J.; Houde, M.; Gabrielsen, G. W.; Berger, U.; Haukås, M.; Letcher, R. J.; Muir, D. C. G. Perfluorinated Alkyl Substances in Plasma, Liver, Brain, and Eggs of Glaucous Gulls (*Larus Hyperboreus*) from the Norwegian Arctic. *Environ. Sci. Technol.* **2005**, *39*, 7439–7445.
- (9) Kucharzyk, K. H.; Darlington, R.; Benotti, M.; Deeb, R.; Hawley, E. Novel Treatment Technologies for PFAS Compounds: A Critical Review. *J. Environ. Manage.* **2017**, *204*, 757–764.
- (10) Liu, J.; Qu, R.; Wang, Z.; Mendoza-Sanchez, I.; Sharma, V. K. Thermal- and Photo-Induced Degradation of Perfluorinated Carboxylic Acids: Kinetics and Mechanism. *Water Res.* **2017**, *126*, 12–18.
- (11) Bentel, M. J.; Yu, Y.; Xu, L.; Li, Z.; Wong, B. M.; Men, Y.; Liu, J. Defluorination of Per- and Polyfluoroalkyl Substances (PFASs) with Hydrated Electrons: Structural Dependence and Implications to PFAS Remediation and Management. *Environ. Sci. Technol.* **2019**, *53*, 3718–3728.
- (12) Bentel, M. J.; Yu, Y.; Xu, L.; Kwon, H.; Li, Z.; Wong, B. M.; Men, Y.; Liu, J. Degradation of Perfluoroalkyl Ether Carboxylic Acids with Hydrated Electrons: Structure-Reactivity Relationships and Environmental Implications. *Environ. Sci. Technol.* **2020**, *54*, 2489–2499.
- (13) Krusic, P. J.; Roe, D. C. Gas-Phase NMR Technique for Studying the Thermolysis of Materials: Thermal Decomposition of Ammonium Perfluoroctanoate. *Anal. Chem.* **2004**, *76*, 3800–3803.
- (14) Krusic, P. J.; Marchione, A. A.; Roe, D. C. Gas-Phase NMR Studies of the Thermolysis of Perfluoroctanoic Acid. *J. Fluor. Chem.* **2005**, *126*, 1510–1516.
- (15) Stockenhuber, S.; Weber, N.; Dixon, L.; Lucas, J.; Grimison, C.; Bennett, M.; Stockenhuber, M.; Mackie, J.; Kennedy, E. Thermal Degradation of Perfluoroctanoic Acid (PFOA). *16th International Conference on Environmental Science and Technology*; Royal Society of Chemistry, 2019; pp 1–3.
- (16) Lazerte, J. D.; Hals, L. J.; Reid, T. S.; Smith, G. H. Pyrolyses of the Salts of the Perfluoro Carboxylic Acids. *J. Am. Chem. Soc.* **1953**, *75*, 4525–4528.
- (17) Altarawneh, M. A Theoretical Study on the Pyrolysis of Perfluorobutanoic Acid as a Model Compound for Perfluoroalkyl Acids. *Tetrahedron Lett.* **2012**, *53*, 4070–4073.
- (18) Altarawneh, M.; Almatarneh, M. H.; Dlugogorski, B. Z. Thermal Decomposition of Perfluorinated Carboxylic Acids: Kinetic Model and Theoretical Requirements for PFAS Incineration. *Chemosphere* **2022**, *286*, 131685.
- (19) Wallace, S.; Lambrakos, S.; Shabaev, A.; Massa, L. Calculated IR Absorption Spectra for Perfluoroalkyl and Polyfluoroalkyl (PFAS) Molecules. *Struct. Chem.* **2021**, *32*, 899–907.
- (20) Rayne, S.; Forest, K. Comparative Semiempirical, Ab Initio, and Density Functional Theory Study on the Thermodynamic Properties of Linear and Branched Perfluoroalkyl Sulfonic Acids/Sulfonyl Fluorides, Perfluoroalkyl Carboxylic Acid/Acyl Fluorides, and Perhydroalkyl Sulfonic Ac. *J. Mol. Struct. THEOCHEM* **2010**, *941*, 107–118.
- (21) Rayne, S.; Forest, K. Theoretical Studies on the PKa Values of Perfluoroalkyl Carboxylic Acids. *J. Mol. Struct. THEOCHEM* **2010**, *949*, 60–69.
- (22) Chen, Y.; Ma, H.; Zhu, J.; Gu, Y.; Liu, T. New Insights into Ferric Iron-Facilitated UV 254 Photolytic Defluorination of Perfluoroctanoic Acid (PFOA): Combined Experimental and Theoretical Study. *J. Hazard. Mater.* **2022**, *434*, 128865.
- (23) Bao, Y.; Deng, S.; Jiang, X.; Qu, Y.; He, Y.; Liu, L.; Chai, Q.; Mumtaz, M.; Huang, J.; Cagnetta, G.; et al. Degradation of PFOA Substitute: GenX (HFPO-DA Ammonium Salt): Oxidation with UV/Persulfate or Reduction with UV/Sulfite? *Environ. Sci. Technol.* **2018**, *52*, 11728–11734.
- (24) Qu, R.; Liu, J.; Li, C.; Wang, L.; Wang, Z.; Wu, J. Experimental and Theoretical Insights into the Photochemical Decomposition of Environmentally Persistent Perfluorocarboxylic Acids. *Water Res.* **2016**, *104*, 34–43.
- (25) Chai, J.; Head-Gordon, M. Long-Range Corrected Hybrid Density Functionals with Damped Atom – Atom Dispersion Corrections *W. Phys. Chem. Chem. Phys.* **2008**, *10*, 6615–6620.
- (26) Curtiss, L. A.; Raghavachari, K.; Redfern, P. C.; Rassolov, V.; Pople, J. A. Gaussian-3 (G3) Theory for Molecules Containing First and Second-Row Atoms. *J. Chem. Phys.* **1998**, *109*, 7764–7776.
- (27) Curtiss, L. A.; Raghavachari, K.; Redfern, P. C.; Baboul, A. G.; Pople, J. A. Gaussian-3 Theory Using Coupled Cluster Energies. *Chem. Phys. Lett.* **1999**, *314*, 101–107.
- (28) Frisch, M.; Trucks, G.; Schlegel, H.; Scuseria, G.; Robb, M.; Cheeseman, J.; Scalmani, G.; Barone, V.; Mennucci, B.; Petersson, G. A.; et al. *Gaussian 09*, Revision D.01; Gaussian, Inc.: Wallingford, CT, 2009.

(29) Werner, H.-J.; Knowles, P. J.; Knizia, G.; Manby, F. R.; Schütz, M. Molpro: A General-Purpose Quantum Chemistry Program Package. *WIREs Comput. Mol. Sci.* **2012**, *2*, 242–253.

(30) Fukui, K. The Path of Chemical Reactions — The IRC Approach. *Acc. Chem. Res.* **1981**, *14*, 363–368.

(31) Hratchian, H. P.; Schlegel, H. B. Using Hessian Updating To Increase the Efficiency of a Hessian Based Predictor-Corrector Reaction Path Following Method. *J. Chem. Theory Comput.* **2005**, *1*, 61–69.

(32) Hanwell, M. D.; Curtis, D. E.; Lonie, D. C.; Vandermeersch, T.; Zurek, E.; Hutchison, G. R. Avogadro: An Advanced Semantic Chemical Editor, Visualization, and Analysis Platform. *J. Cheminform.* **2012**, *4*, 1–17.

(33) Avogadro: An Open-Source Molecular Builder and Visualization Tool; <https://avogadro.cc/>.

(34) Tumanov, V. E.; Denisov, E. T. Estimation of the Dissociation Energies of O–O, C–O, and O–H Bonds in Acyl Peroxides, Acids, and Esters from Kinetic Data on the Degradation of Diacyl Peroxides. *Pet. Chem.* **2005**, *45*, 237–248.

(35) In *L'analyse de l'eau*, 9th ed.; Rodier, J., Legube, B., Merlet, N., Eds.; DUNOD: Paris, France, 2009.

(36) Van Hoomissen, D. J.; Vyas, S. 1,2-Fluorine Radical Rearrangements: Isomerization Events in Perfluorinated Radicals. *J. Phys. Chem. A* **2017**, *121*, 8675–8687.

(37) Cramer, C. J. *Essential of Computational Chemistry: Theories and Models*, 2nd ed.; John Wiley and Sons, Ltd.: Chichester, England, 2004.

(38) Ratkiewicz, A.; Truong, T. N. Kinetics of the C–C Bond Beta Scission Reactions in Alkyl Radical Reaction Class. *J. Phys. Chem. A* **2012**, *116*, 6643–6654.

(39) Sansotera, M.; Persico, F.; Rizzi, V.; Panzeri, W.; Pirola, C.; Bianchi, C. L.; Mele, A.; Navarrini, W. The Effect of Oxygen in the Photocatalytic Oxidation Pathways of Perfluoroctanoic Acid. *J. Fluor. Chem.* **2015**, *179*, 159–168.

(40) Tsang, W.; Burgess, D. R.; Babushok, V. On the Incinerability of Highly Fluorinated Organic Compounds. *Combust. Sci. Technol.* **1998**, *139*, 385–402.

(41) Arsenault, G.; McAlees, A.; McCrindle, R.; Riddell, N. Analysis of Perfluoroalkyl Anion Fragmentation Pathways for Perfluoroalkyl Carboxylates and Sulfonates during Liquid Chromatography/Tandem Mass Spectrometry: Evidence for Fluorine Migration Prior to Secondary and Tertiary Fragmentation. *Rapid Commun. Mass Spectrom.* **2007**, *21*, 3803–3814.

(42) Singh, R. K.; Ruij, B.; Sadhukhan, A. K.; Gupta, P. Thermal Degradation of Waste Plastics under Non-Sweeping Atmosphere: Part 1: Effect of Temperature, Product Optimization, and Degradation Mechanism. *J. Environ. Manage.* **2019**, *239*, 395–406.

(43) Wang, J.; Lin, Z.; He, X.; Song, M.; Westerhoff, P.; Doudrick, K.; Hanigan, D. Critical Review of Thermal Decomposition of Per- and Polyfluoroalkyl Substances: Mechanisms and Implications for Thermal Treatment Processes. *Environ. Sci. Technol.* **2022**, *56*, 5355–5370.

(44) Matula, R. A. The Thermal Decomposition of Perfluoropropene. *J. Phys. Chem.* **1968**, *72*, 3054–3056.

(45) Feller, D.; Peterson, K. A.; Dixon, D. A. Ab Initio Coupled Cluster Determination of the Heats of Formation of  $C_2H_2F_2$ ,  $C_2F_2$ , and  $C_2F_4$ . *J. Phys. Chem. A* **2011**, *115*, 1440–1451.

(46) Baird, N. C.; Taylor, K. F. Multiplicity of the Ground State and Magnitude of the T1–S0 Gap in Substituted Carbenes. *J. Am. Chem. Soc.* **1978**, *100*, 1333–1338.

(47) Blanksby, S. J.; Ellison, G. B. Bond Dissociation Energies of Organic Molecules. *Acc. Chem. Res.* **2003**, *36*, 255–263.

## □ Recommended by ACS

### Thermal Decomposition of Perfluoroctanesulfonic Acid (PFOS) in the Presence of Water Vapor

Nathan H. Weber, Eric M. Kennedy, et al.

OCTOBER 07, 2022

INDUSTRIAL & ENGINEERING CHEMISTRY RESEARCH

READ 

### Volatility and Nonspecific van der Waals Interaction Properties of Per- and Polyfluoroalkyl Substances (PFAS): Evaluation Using Hexadecane/Air Partition Coefficients

Jort Hammer and Satoshi Endo

OCTOBER 14, 2022

ENVIRONMENTAL SCIENCE & TECHNOLOGY

READ 

### The Need for Testing Isomer Profiles of Perfluoroalkyl Substances to Evaluate Treatment Processes

Kaushik Londhe, Arjun K. Venkatesan, et al.

OCTOBER 31, 2022

ENVIRONMENTAL SCIENCE & TECHNOLOGY

READ 

### Widening the Lens on PFASs: Direct Human Exposure to Perfluoroalkyl Acid Precursors (pre-PFAAs)

Carrie A. McDonough, Jamie C. DeWitt, et al.

MARCH 24, 2022

ENVIRONMENTAL SCIENCE & TECHNOLOGY

READ 

Get More Suggestions >